Modifying materials by intercalation

By inserting layers of guest molecules into anisotropic materials such as graphite, materials scientists are producing compounds with controlled electronic, magnetic, structural and thermal properties.

Mildred S. Dresselhaus

For the past decade, materials research has focused on synthesizing new materials and generating new structural arrangements that exhibit specific desired properties. Some of the greatest advances in this area have come out of work on intercalation compounds,[1–5] which are formed by the insertion of atomic or molecular layers of a guest chemical species—an intercalant—between layers in a host material. Figure 1 illustrates the basic structure of intercalation compounds. Part **a** of the figure depicts graphite intercalated with lithium; this structure is described as "commensurate," because the atoms in each layer of guest material are in registry with those in the neighboring layers of the host material. Part **b** of the figure shows the incommensurate nature of graphite intercalated with ferric chloride. Although graphite intercalation compounds have been synthesized for over 150 years, it is only very recently that methods have been perfected to the point that one can prepare materials with specific structures and properties. These advances in materials synthesis, coupled with current theoretical interest in two-dimensional physics, have contributed to the current high level of interest in graphite intercalation compounds.

Because of their unusual ordering, intercalation compounds offer opportunities for the study of new types of phenomena. For example, novel phase transitions arise through the "staging" phenomenon, in which a constant number of layers of host material are sandwiched between sequential intercalate layers, as figure 2 shows. This phenomenon gives a periodic array of intercalate sheets that can independently undergo two-dimensional order–disorder and structural phase transitions. Staging allows one to control the separation between the intercalation layers, and thereby to produce systems in which it might be possible to study two-dimensional magnetism or two-dimensional superconductivity. The current growing interest in submicron technology has also drawn attention to graphite intercalation compounds and their natural submicron structures. Intensive studies of intercalation compounds are now under way in many places, and in the next few years we can expect to see great progress in understanding these materials and in utilizing their special properties.

In this article, I describe how intercalation compounds are synthesized and how their structures are determined, and I will discuss novel structural phase transitions. I look at the electronic structure and the associated unique electrical and thermal transport properties of these new compounds. And I discuss the particularly interesting magnetic and superconducting properties of intercalation compounds. First, however, I give a brief overview of the subject.

Intercalation occurs in highly anisotropic layered structures where the intraplanar binding forces are large in comparison with the interplanar binding forces. The guest species in an intercalation compound exhibits order, whereas the guest species in a doped compound tends to occupy random locations. Examples of host materials for intercalation compounds are graphite[1]—which will serve as the main example in this article—transition metal dichalcogenides,[2] some silicates, and metal chlorides. At present, several hundred different chemical species are known to intercalate into graphite. By varying the intercalant species and concentration, one can prepare a large number of compounds with different properties.

Graphite intercalation compounds exhibit a high degree of ordering. The most striking type of ordering is the staging phenomenon mentioned above, which features a periodic arrangement of n graphite layers between sequential intercalate layers, where n is the "stage index." In practice one can prepare single-staged materials with only small (1% to 5%) admixtures of secondary-staged regions.

The simplest method for determining the staging in graphite intercalation compounds is x-ray diffraction based on $(00l)$ reflections, which shows the superlattice periodicity associated with

Mildred Dresselhaus is professor in the department of electrical engineering and computer science, and in the department of physics, at Massachusetts Institute of Technology, Cambridge. She is president of the American Physical Society.

0031-9228 / 84 / 0300 60–09 / $01.00

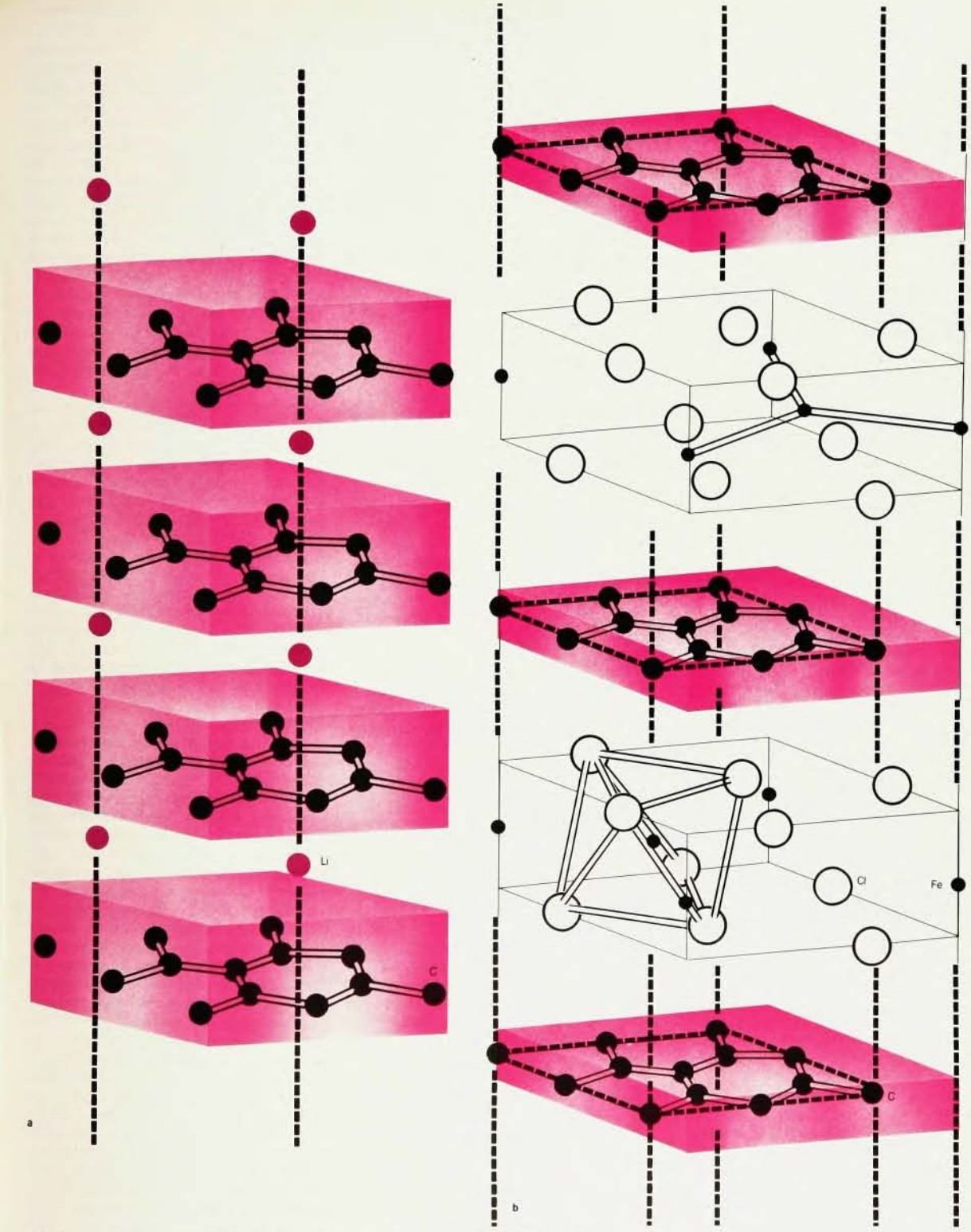

Structure of commensurate (**a**) and incommensurate (**b**) graphite intercalation compounds. The model in **a** shows the stacking of graphite layers and lithium layers in the compound C_6Li. The distance between graphite layers is 3.71 Å; the diamond-shaped segments of graphite layers shown here are 4.92 Å, or $2a_0$, on a side. The compound in **b** is $C_{6.6}$ $FeCl_3$, in which the graphite layers are 9.37 Å apart. The intraplane separation of carbon atoms is the same as in **a**; the lattice constants for the $FeCl_3$ layers are nearly the same as those in pristine $FeCl_3$.

Figure 1

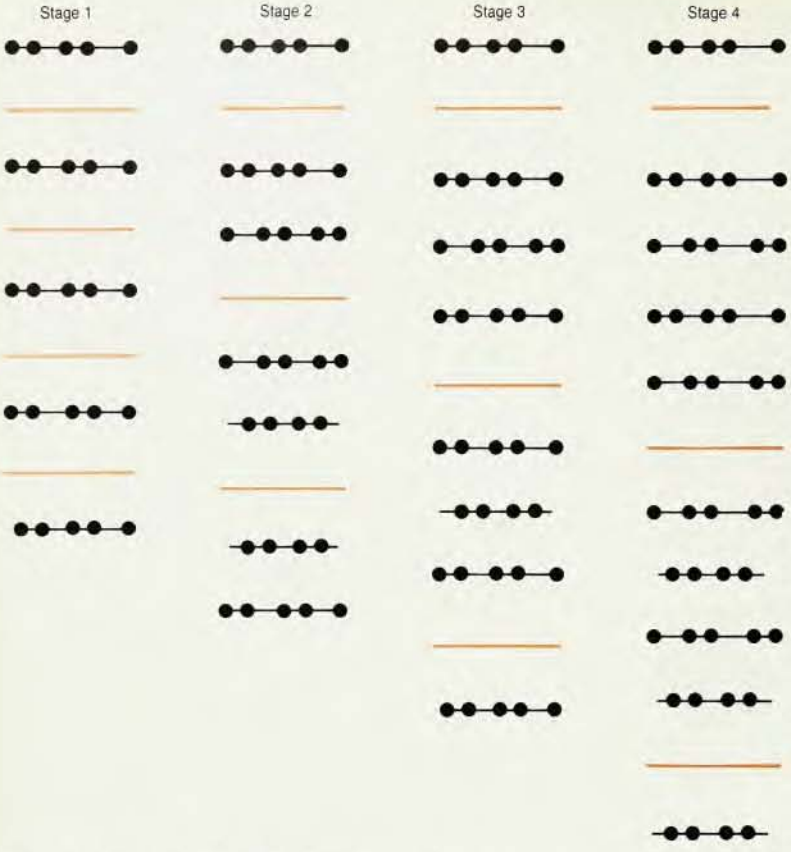

Staging phenomenon. This schematic diagram shows the arrangement of layers in four potassium-intercalated graphite compounds. Solid lines connecting circles represent graphite layers, with the positions of the circles indicating schematically the projected positions of the carbon atoms. The colored lines represent potassium layers. In the stage-one compound, layers of graphite and potassium alternate. In stage-n compounds, there are n graphite layers between successive potassium layers. Graphite layers between potassium layers maintain an alternating pattern of registration, as indicated. The distances I_c between adjacent potassium layers in the stage-one through stage-four compounds represented here are 5.35 Å, 8.75 Å, 12.10 Å and 15.44 Å, respectively. Potassium layers in the stage-one compound arrange themselves in a sequence of four orientations. Figure 2

staging. Diffractograms show that well-staged materials can be prepared with stage indices up to about 10, indicating a c-axis repeat distance I_c (see figure 2) between consecutive intercalate layers of about 40 Å. The physical basis for the staging phenomenon is the strong interatomic intercalate–intercalate binding relative to the intercalate–graphite binding, thereby favoring a close-packed in-plane intercalate arrangement. The introduction of each intercalate layer adds a substantial strain energy as the crystal expands to accommodate the intercalate layer, thereby favoring the insertion of a minimum number of intercalate layers, consistent with a given average intercalate concentration. Thus the state of minimum energy corresponds to a close-packed in-plane intercalate arrangement and the minimum number of intercalate layers, with the largest possible separation between sequential intercalate layers for a given intercalate concentration. This combination of conditions results in staging.

Analysis of (00l) x-ray diffractograms for many graphite intercalation compounds shows that the repeat distance I_c has the simplest possible stage dependence

$$I_c = d_s + (n-1)\,c_0$$

Here d_s is the distance between two graphite layers between which an intercalate layer is sandwiched, n is the stage index and c_0 is the interlayer separation in pristine graphite. The relative intensities of the (00l) diffraction peaks give information on the in-plane intercalate density. In the case of multiple-layer intercalates, the peak intensities also provide information on the separation of layers within the intercalate sandwich, and on the separation between the intercalate and adjacent graphite layers. For example, the system of graphite intercalated with iron chloride, shown in figure 1b, forms a three-layer intercalate structure consisting of an iron layer surrounded by two chlorine layers that interface with the graphite. The table on page 66 gives values for the intercalate sandwich thickness d_s for a number of graphite intercalation compounds. In general, one can obtain the repeat distances I_c using these values and the above equation.

We can use the staging phenomenon to control the distance between sequential intercalate layers. Staging thus gives us a mechanism for controlled variation of the physical properties of the compounds. For example, if the intercalant results in a magnetic or superconducting compound, the staging phenomenon then permits study of the magnetism or superconductivity as the interplanar magnetic interaction or the c-axis superconducting coherence distance decreases in a controlled manner. This allows us to study the transition from three-dimensional to two-dimensional behavior.

Synthesis

One can bring about intercalation starting from a solid, liquid or gaseous guest material,[6] though intercalation from the vapor or from solution is most common. Electrochemical techniques are also employed. It is often possible to prepare a given intercalation compound by more than one technique. Generally, one intercalates simple molecules from the vapor, using a two-zone furnace, and larger organic molecules from solution. The intercalation rate and resulting intercalate concentration (or stage) depend strongly on conditions such as the pressure, the ambient temperature, the temperature difference between the host material and the intercalant, the physical dimensions of the sample of host material, and the defect density and degree of crystalline order in the host material. When intercalating from the vapor, the initiation of the intercalation process requires the partial pressure of the intercalate to exceed a threshold value that depends on temperature, structure of the host material and the intercalate species. The process proceeds with the insertion of intercalate layers sequentially from the surface layers inward, but starting from the edges and advancing into the layer planes.

One can introduce interesting inter-

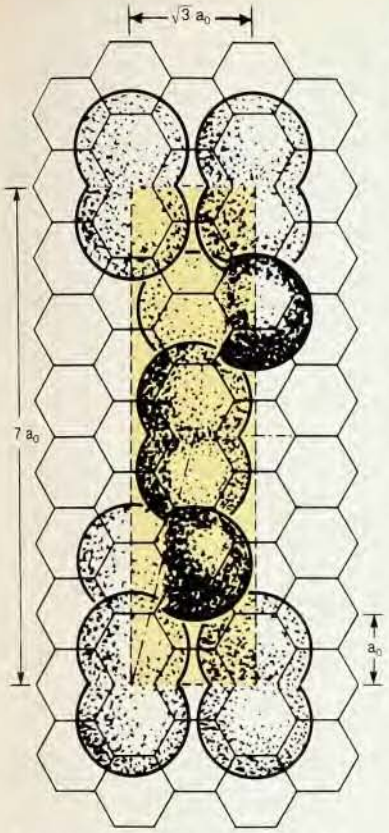

In-plane structure of an intercalate. This diagram shows the lattice of the two-dimensional intercalate Br_2 projected onto the hexagonal network of graphite, with which it is commensurate. The colored region represents the bromine layer's rectangular unit cell, whose length and width are 17.22 Å and 4.26 Å, respectively. Figure 3

calants such as hydrogen, mercury or benzene into a graphite host through stepwise intercalation, in which the graphite is first intercalated with an alkali metal such as potassium. Interestingly, the potassium–hydrogen graphite intercalation compounds allow a packing density of hydrogen atoms comparable to that in solid hydrogen; potassium–mercury graphite intercalation compounds are of interest for their anisotropic superconducting properties; and the potassium–benzene graphite intercalation compounds exhibit catalytic behavior.

Graphite intercalation compounds are generally very reactive and must be stored in an inert atmosphere or encapsulated in glass ampoules. However, a few of the graphite compounds, such as those with the intercalants $FeCl_3$ and $SbCl_5$, are quite stable in air.

By allowing the introduction of new species and the creation of novel structures, intercalation gives us a method for modifying drastically the structure and therefore the properties of the host material. Of particular interest to physicists is the synthesis of new classes of anisotropic materials, some of which exhibit quasi-two-dimensional structure and properties.

Structure

The principal technique for the structural characterization of graphite intercalation compounds is x-ray diffraction, which is used primarily to determine the stage index. Electron diffraction is particularly useful for determining in-plane ordering, while elastic neutron scattering gives information on the stage index and on the interplanar intercalate stacking arrangement.

The desire to understand phase transitions associated with the basal plane structure has motivated many of the recent structural studies on graphite intercalation compounds. The primary mechanism for in-plane structural phase transitions in graphite intercalation compounds is differential in-plane thermal expansion. The intercalate–intercalate bonding is much stronger than the intercalate–graphite bonding, and results in a large thermal expansion of the intercalate layer relative to that of the graphite layer, which exhibits almost no thermal expansion. Thus, if a particular intercalate layer is commensurate with the adjacent graphite layer at some temperature, the differential thermal expansion can give rise to a transition to an incommensurate phase at higher or lower temperatures.

The simplest experimental technique for identifying phase transitions is to measure transport properties, such as electrical resistance, as a function of temperature.[7] The transport properties characteristically show anomalies at the phase-transition temperature, reflecting changes in the scattering processes at the phase transition. For more detailed information on the nature of structural phase transitions, one can carry out x-ray, electron or neutron diffraction measurements.

Graphite intercalation compounds are an attractive class of materials for investigating phase transitions in two-dimensional systems. A novel example of such a phase transition is found in the graphite–bromine system,[7] which upon heating exhibits a phase transition from a commensurate structure to a special kind of incommensurate phase. At yet higher temperatures there is two-dimensional melting.

Figure 3 shows the commensurate in-plane structure of a stage-four graphite–Br_2 compound at room temperature. The intercalate basis vector of length $\sqrt{3}\,a_0$ in the figure is at 30° with respect to one of the graphite basis vectors, and the superlattice basis vector of length $7a_0$ is parallel to the other graphite basis vector. The very high thermal expansion coefficient of solid bromine relative to that of graphite in the basal plane suggests that there should be a transition to an incommensurate intercalate phase at some elevated temperature.

Experimenters have, in fact, observed a transition to an incommensurate phase in the stage-four graphite–bromine compound $C_{28}Br_2$ at a temperature of 69.05 °C, but the transition is to a special structure called a "stripe domain" incommensurate phase. In this phase, the lattice constant remains commensurate in the $\sqrt{3}$-fold direction, that is, the direction of the basis vector of length $\sqrt{3}a_0$. However, in the 7-fold direction, the lattice remains locally commensurate, but after N unit cells there is a phase slip of $2b/7$ (see figure 4), where b, which is $7a_0$, is the lattice constant of the commensurate superlattice in the long direction.

As the temperature increases beyond the transition temperature T_c, the intercalate becomes increasingly incommensurate by decreasing the number N of unit cells between phase slips. To establish the quantitative structure of the incommensurate stripe-domain phase, one can perform detailed high-resolution x-ray scattering experiments.[7] In such experiments, one sees the transition to the incommensurate stripe-domain phase as the onset of a

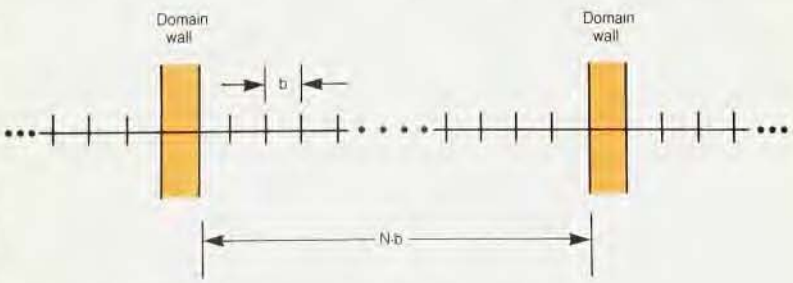

Stripe-domain model proposed for stage-four Br_2-intercalated graphite. The intercalate lattice remains commensurate except for a phase slip in one direction every N unit cells. Figure 4

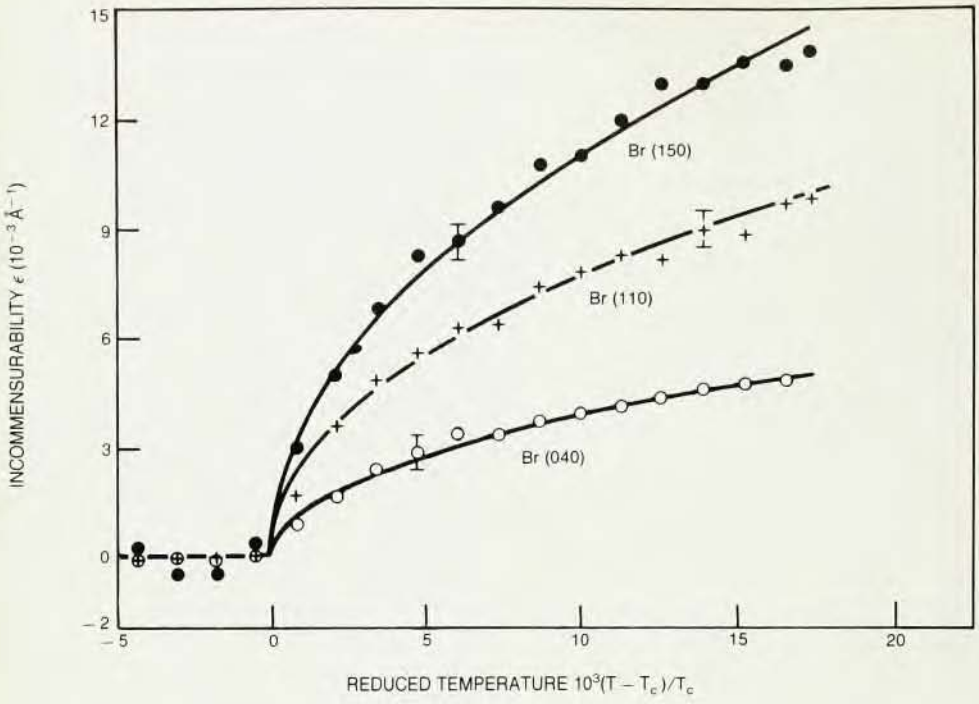

Incommensurability as a function of temperature. Data points show that the lattice of the intercalate bromine loses registry with that of the graphite host as the temperature moves beyond the critical temperature T_c. The solid curves represent power-laws fits with exponent 0.5. (From reference 7.) Figure 5

modulated diffraction pattern in which the dominant bromine superlattice diffraction spots are shifted in the 7-fold direction. There is no shift of the bromine superlattice spots in the $\sqrt{3}$-fold direction. There is also no change in the diffraction spots for the graphite host at the phase transition.

Physicists at the Landau Institute of Theoretical Physics have given[8] a detailed theory for a one-dimensional commensurate–incommensurate transition in a two-dimensional lattice. They predict that the domain-wall density and hence the incommensurability ϵ should initially rise as $(T - T_c)^{1/2}$ but should saturate as the domain-wall density increases. Experimental results for stage-four bromine-intercalated graphite show just this behavior near the transition temperature T_c, with an exponent of 0.50 ± 0.02. This is shown in figure 5, where data for the incommensurability ϵ were fit to the functional form $\epsilon = \epsilon_0[(T - T_c)/T_c]^{\beta}$, with $\beta = 0.5$, for the Br (110) peak; with this functional form, excellent agreement was also obtained for the Br (150) and Br (040) peaks with no adjustable parameters. The positions of the x-ray superlattice peaks from the incommensurate lattice, and the intensities of those peaks, are well described by a model that features sharp domain walls with widths of less than one unit cell.

As the temperature of the stage-four sample increases further, the intercalate layer undergoes a continuous anisotropic two-dimensional melting transition at 102.25 °C, also identified by analysis of the high-resolution x-ray scattering lineshapes. The results show the retention of substantial order in the $\sqrt{3}$-fold direction upon melting.

High-resolution x-ray scattering measurements[7] on bromine-intercalated graphite give direct evidence that in-plane coherence distances are long—about 10^4 Å. Although some intercalates, such as KHg and Br_2, exhibit large in-plane defect-free regions, other intercalates show island structures. Such island structures commonly occur with intercalates that form incommensurate in-plane structures and with those that exhibit "disproportionation" phenomena. Disproportionation is the process in which the intercalation of one chemical species results in the formation of new chemical species inside the host material.[9] For example, the introduction of $SbCl_5$ into graphite apparently results in the formation of some $SbCl_3$ and $SbCl_6^-$. Researchers expect the presence of intercalate island structures to appear as line broadening in spectra and as additional scattering channels that affect the transport properties.

Electronic structure

Intercalation in graphite does not significantly change the in-plane ordering in the layers of the host material, nor does it change the interlayer spacing between these layers. This suggests that the electronic and lattice-mode structures for graphite intercalation compounds are closely related to those of layers of the host and intercalate materials. Investigations of the electronic and lattice properties of graphite intercalation compounds show that the perturbation introduced by the intercalate layers is largely confined to the two graphite bounding layers—the graphite layers that are adjacent to the intercalate layer—while the *interior* layers of graphite are largely unperturbed. Also, numerous experiments show similarities between the structural ordering of the intercalate layer and the structural ordering of the corresponding layer of the parent intercalate material. Thus, calculations of the electronic dispersion relations for intercalation compounds are based on a hybridization of the electronic levels for the two parent materials. For example, the electronic dispersion relations for C_8K (stage-one potassium-intercalated graphite) exhibit[10] graphitic energy bands very similar to those in pristine graphite, as well as intercalate s and p bands readily identified with pristine potassium. Matters are further simplified by considering the *symmetry* of the intercalation compound. The superlattice symmetry due to staging introduces zone-folding effects that have an important bearing on the form of the electronic energy-band and lattice-mode structures. Some theorists have carried out detailed "first principles" band calculations for several graphite intercalation compounds and others have developed phenomenological energy-band models based on crystal sym-

metry and measurements of experimental properties.[11]

The large anisotropy in electronic properties is due to the extremely small dispersion along the c-axis and the high level of dispersion in the layer planes—the energy-versus-wavevector curves are nearly linear for bands near the Fermi level. Furthermore, the density of states in pristine graphite is very small near the Fermi level. Because intercalation of graphite causes a large increase in its carrier density, the Fermi level moves well into the conduction band for donors and well into the valence band for acceptors, thus giving rise to a large increase in the density of states for both donors and acceptors.

Electronic and thermal transport

Intercalation causes large changes in electron concentration because of the transfer of charge between the intercalate and host. The conductivity model in figure 6 explains this, showing schematically the charge transfer in the case of a donor intercalate in graphite. Suppose, for example, that the intercalant species is the alkali metal potassium. Each potassium atom has one valence electron. If this electron is transferred to the graphite layers, the intercalate layer becomes positively charged, thereby attracting electrons in the graphite layers. Thus most of the transferred charge resides in the graphite bounding layers. Because the in-plane intercalate concentration is typically a factor of 10 less than the carbon concentration in a graphite layer, one can achieve an increase as large as three orders of magnitude in the carrier concentration in potassium-intercalated graphite compared with pristine graphite.

Thus, intercalation results in major changes in the transport properties.[12] The in-plane electrical conductivity σ_a increases from that for graphite by an order of magnitude or more, as figure 7 shows for several alkali metal graphite intercalation compounds.[13] The magnitude of the increase in the in-plane conductivity depends on the intercalate species and its concentration. Of the various types of layers within the unit cell (see figure 6), the graphite bounding layers contribute most to the conductivity because these layers have a high carrier density relative to that in the graphite interior layers and a very high carrier mobility relative to that in the intercalate layers. Though smaller, the contribution to the conductivity of the graphite interior layers can in some cases be significant. We can account qualitatively for the observed stage dependence of the in-plane conductivity by considering the conductance of the total sample as a sum of the conductances of the individual layer types, weighted according to their relative thicknesses within the unit cell.

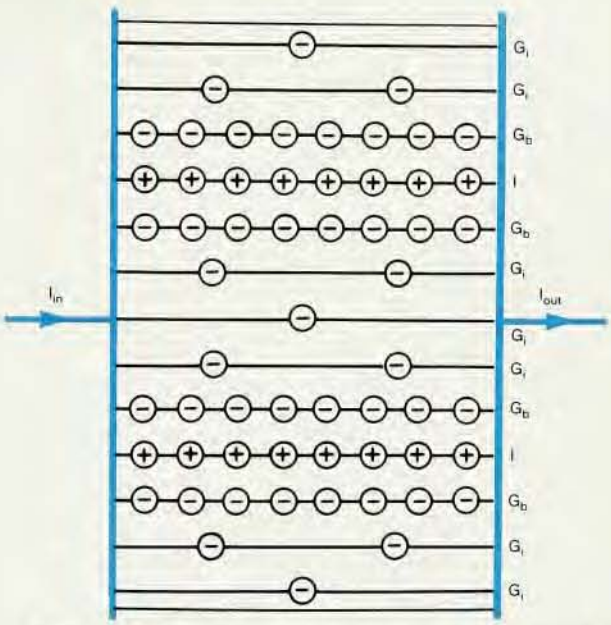

Additive conductance model for graphite intercalation compounds. Labeled are the graphite interior layers (G_i), graphite bounding layers (G_b) and intercalate layers (I). The figure indicates schematically the electronic charge distribution for a stage-five donor compound. Figure 6

Hall-effect measurements show that the sign of the dominant carrier is positive (for acceptors) or negative (for donors). Thus, intercalation can increase the number of donors and cause the Fermi level to rise, or increase the number of acceptors and cause the Fermi level to fall. It is believed that the alkali metal intercalates donate essentially all their free carriers to the graphite layers for the higher stage compounds—those with stage index $n \geq 2$. The carrier density decreases rapidly with distance into the graphite interior layers.

The charge transfer in donor compounds is often less than one electron per intercalate unit but generally is greater than for acceptor compounds. For the acceptor compounds, the intercalate layer becomes negatively charged by extracting electrons predominantly from the graphite bounding layers, in contrast to the situation shown in figure 6 for the donor compounds. Thus, the graphite bounding layers have a high concentration of holes for the acceptor compounds.

Although the c-axis conductivity σ_c also increases with increasing intercalate concentration for donor compounds, it decreases in the case of acceptor compounds, often resulting in materials with an electrical conductivity anisotropy ratio σ_a/σ_c in excess of about 10^6. This wide range of behavior in electrical conductivity occurs because intercalation increases the carrier density while decreasing the carrier mobility, and because the graphite–intercalate interaction varies significantly from one intercalant to another.

As the temperature is lowered, the in-plane electrical conductivity increases, with the effect being larger for donors than for acceptors. At low temperature, graphite intercalation compounds normally have a scattering time much larger than the reciprocal of the cyclotron frequency, so that electrons can complete at least one orbit before scattering. Thus, one can readily observe quantum oscillatory phenomena in both donor and acceptor graphite intercalation compounds at low temperatures. Such observations yield direct information on the shape of the Fermi surface and on the carrier density, independent of scattering processes and scattering times.[14] Experimental results show that intercalation greatly increases the size of the Fermi surface and causes the formation of numerous carrier pockets. The Fermi surface for the graphitic electrons tends to be cylindrical in shape, so that the electrons exhibit essentially infinite effective masses along the c-axis, and quasi-two-dimensional transport behavior.

Thermal transport properties of graphite intercalation compounds are highly anisotropic,[15] as are the optical properties.[1,12] Although the lattice contribution dominates the thermal conductivity in the host crystal, the great

increase in carrier concentration in graphite intercalation compounds allows the electronic contribution to dominate the thermal conductivity at low temperatures, that is, at temperatures below 10 K. Because of the increase in scattering due to the increased concentration of defects, intercalation decreases the absolute magnitude of the room-temperature thermal conductivity. The Wiedemann–Franz relation (which relates the low-temperature electrical conductivity to the low temperature electronic contributions to thermal conductivity) is satisfied for graphite intercalation compounds, and provides an independent method for determining their electrical conductivity in the low-temperature, residual-resistivity range.

Intercalation has very little effect on the anisotropy in the thermal conductivity of graphite at room temperature—that is, the ratio of the room-temperature a-axis and c-axis thermal conductivities is almost unaltered by intercalation. At low temperatures, the electronic contribution to the c-axis thermal conductivity is insignificant because of the low electrical mobility along the c-axis. Thus, the c-axis thermal conductivity is dominated by the phonon contribution throughout the entire temperature range, so that at low temperatures, intercalated graphite exhibits thermal conduction by electrons in the layer planes and by phonons along the c-axis. Because graphite intercalation compounds have a relatively high carrier mobility, one can determine the electronic and lattice contributions to the thermal conductivity independently by applying a high magnetic field to quench the electronic contribution.

The sign of the Seebeck thermoelectric coefficient, or thermopower, for acceptor compounds is positive, and

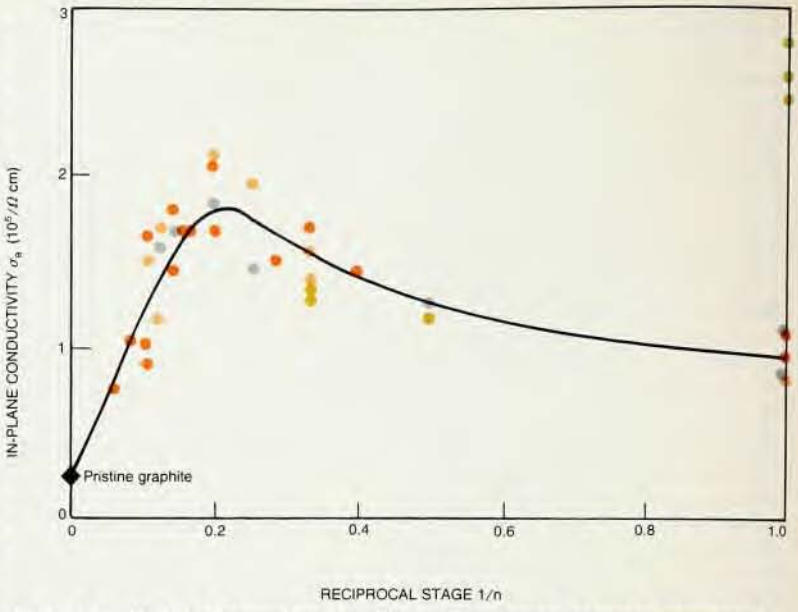

In-plane conductivity of several graphite-alkali metal compounds, plotted as a function of stage. Ochre represents lithium intercalant; light orange, rubidium; dark orange, potassium; gray, cesium. (From reference 13.) Figure 7

that for donor compounds is negative, as expected. The temperature dependence of the in-plane thermopower is similar (except for sign) for donor and acceptor graphite intercalation compounds, but these temperature dependences are very different from that in pristine graphite. Furthermore, the temperature dependence of the thermopower is anisotropic, exhibiting different in-plane and c-axis behaviors.

Magnetic properties

Intercalation significantly modifies the magnetic properties of the graphite host material. The specific behavior that one observes depends strongly on whether or not the intercalant is magnetic, and for the case of nonmagnetic intercalants, the behavior depends on whether the intercalant is a donor or an acceptor. Magnetic intercalants form graphite intercalation compounds that exhibit magnetically ordered phases below a critical magnetic ordering temperature, while nonmagnetic intercalants generally yield graphite intercalation compounds that are diamagnetic or paramagnetic, depending upon whether the intercalant is an acceptor or donor, respectively.

Pristine graphite is a highly diamagnetic material because of the large orbital contribution of the highly mobile electrons and holes. The intercalation of graphite with nonmagnetic acceptor intercalates reduces both the magnitude of the diamagnetism and the anisotropy of the magnetic susceptibility. Nonmagnetic *donor* intercalates have a very large effect on the orbital contribution to the magnetic susceptibility, causing the sign of the susceptibility to change from negative to positive. The largest effect occurs in the lowest stage compounds, where the free-carrier density is largest.[16]

The introduction of magnetic intercalants into graphite results in magnetically ordered compounds. Because of the smaller number of magnetic nearest neighbors, the magnetic ordering temperature of the intercalation compound tends to be lower than that in the parent pristine magnetic material. Experiments have found ordered magnetic phases for both acceptor metal chloride intercalates, such as $FeCl_3$, $FeCl_2$, $CoCl_2$ and $NiCl_2$, and the donor intercalate Eu. Variation of the separation between magnetic intercalate layers by increasing the stage index permits study of the transition from three-dimensional magnetic interactions (stage-one compounds) to two-dimensional magnetism (dilute compounds). Researchers use a variety of experimental techniques[17] to study the magnetic properties of graphite intercalation compounds, including measurements of magnetic susceptibility, magnetization and heat capacity, as well as Mössbauer spectroscopy, and neutron scattering.

Because the nearest-neighbor magnetic interaction for graphite intercalation compounds always involves magnetic species in the same layer plane, even low-stage compounds exhibit quasi-two-dimensional behavior. It is more convenient to study this behavior by analyzing the functional form of the

Intercalate sandwich thicknesses

Intercalant	Sandwich thickness
Li	3.71
K	5.35
Rb	5.65
Cs	5.94
Br_2	7.04
HNO_3	7.84
$HClO_3$	7.94
SO_3	7.96
Cl_2O_7	7.98
AsF_5	8.15
SbF_5	8.46
$FeCl_3$	9.37
$CoCl_2$	9.40
$NiCl_2$	9.40
$SbCl_5$	9.42
$AlCl_3$	9.54
KHg	10.22*

The table lists sandwich thicknesses for graphite intercalation compounds. Except as noted, the sandwich thickness is independent of stage.

With the data in this table and the equation on page 62, one can calculate the repeat distance I_c.

*For stage $n > 3$ the thickness decreases to 9.15 Å.

in-plane magnetic susceptibility (measured with the magnetic field perpendicular to the c-axis) which shows a large peak near the onset of a magnetically ordered state at low temperature.

Of significance is the relatively small stage dependence of the temperature of the peak in-plane magnetic susceptibility. This quasi-independence indicates that the magnetic ordering temperature is determined mainly by exchange interactions between nearest neighbors in the planes. The large increase in the magnitude of the susceptibility as the stage index increases is identified with a transition from three-dimensional behavior for the stage-1 compounds to two-dimensional behavior for the high-stage compounds. Detailed measurements on high-stage magnetic $CoCl_2$-intercalated graphite yield very large values for the susceptibility—larger, in fact, than for a ferromagnetic nickel sphere.[18]

Analyses of magnetic susceptibility, magnetization and neutron scattering experiments show that in the absence of an applied magnetic field, the transition metal chloride acceptor compounds undergo two magnetic phase transitions, at critical temperatures represented by T_{cu} and T_{cl}. At temperatures well above the critical temperature T_{cu}, one sees major deviations from the Curie–Weiss law, in which the susceptibility is inversely proportional to the amount by which the temperature exceeds the upper critical temperature. However, the temperature dependence of the susceptibility above this critical temperature does fit well to a Kosterlitz–Thouless form for a two-dimensional model in which electron spins are random except for being confined to the intercalate plane (see figure 8): The behavior is as $(1/\exp b\sqrt{t})$, where t is the reduced temperature $(T - T_c)/T_c$. This is consistent with the arrangement of the spins in a free, or unbound, vortex. Between the upper and lower critical temperatures, the experimental results are consistent with a two-dimensional bound vortex spin state, with the spins randomly aligned in the basal plane and having no interplanar correlations.[18] As the temperature is lowered below the lower critical temperature T_{cl}, three-dimensional spin correlation appears.

The application of external magnetic fields causes dramatic changes in the susceptibility near the phase transition. Figure 8b illustrates this by showing how the magnitude and functional form of the in-plane magnetic susceptibility change when fields as small as 400 Oe are applied parallel to the c-axis. The external field competes with the six-fold symmetry-breaking anisotropy field from the graphite, and suppresses the phase transition, as predicted theoretically by the Koster-

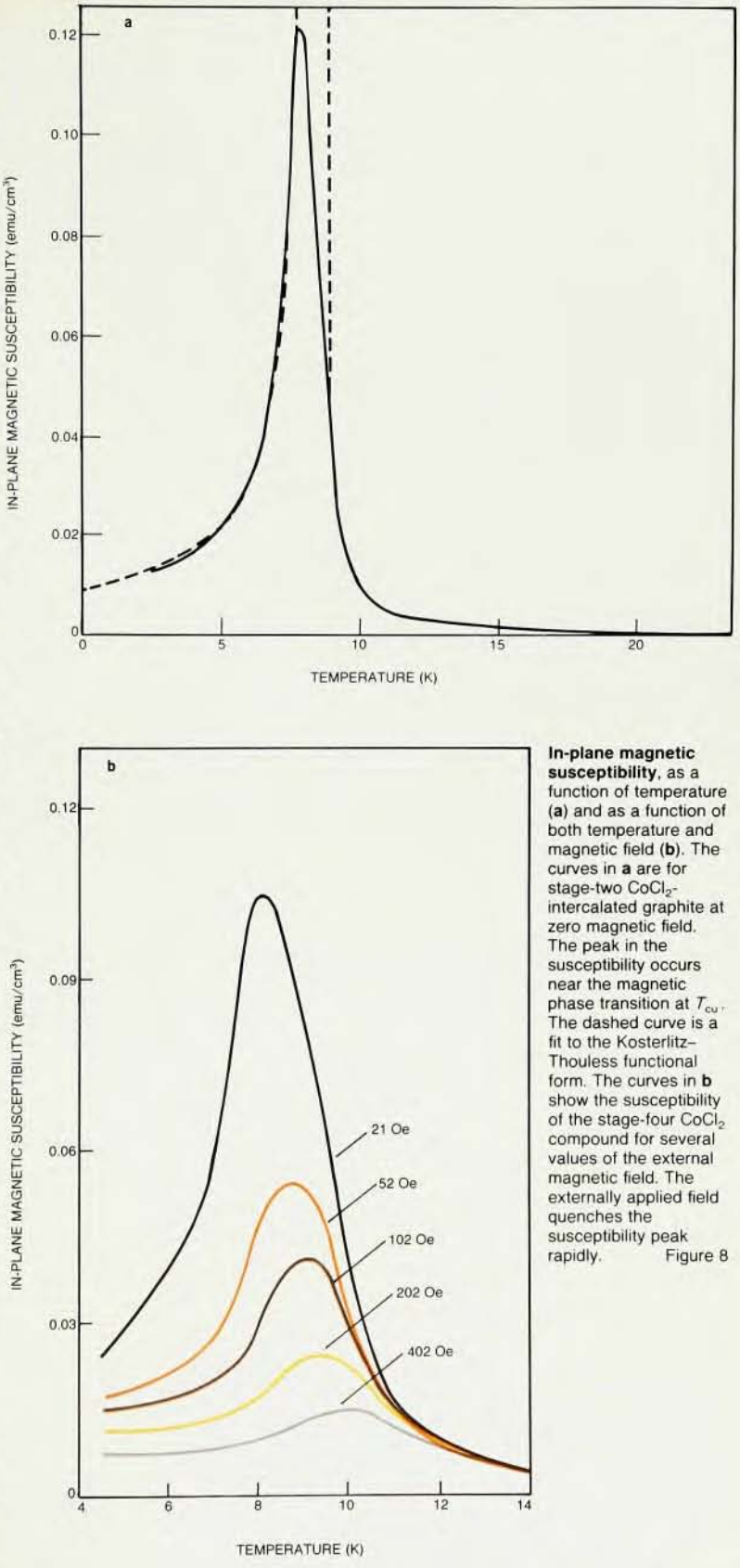

In-plane magnetic susceptibility, as a function of temperature (**a**) and as a function of both temperature and magnetic field (**b**). The curves in **a** are for stage-two $CoCl_2$-intercalated graphite at zero magnetic field. The peak in the susceptibility occurs near the magnetic phase transition at T_{cu}. The dashed curve is a fit to the Kosterlitz–Thouless functional form. The curves in **b** show the susceptibility of the stage-four $CoCl_2$ compound for several values of the external magnetic field. The externally applied field quenches the susceptibility peak rapidly. Figure 8

litz–Thouless theory.

Also of research interest is the high anisotropy of the magnetic susceptibility, which decreases rapidly in amplitude as the probing magnetic field H is rotated from being perpendicular to the c-axis to being parallel to it; when H is parallel to the c-axis, the peak in the susceptibility is quenched. The detailed spin arrangements and magnetic phase diagrams for the magnetic intercalation compounds have yet to be firmly established.

Superconductivity

Intercalation compounds also have particularly interesting superconducting properties.[19] For example, in all cases the critical magnetic fields are highly anisotropic. Also, the first-stage intercalation compound with potassium—C_8K—is found to exhibit a sharp Meissner effect—the expulsion of magnetic flux—at a temperature of about 150 mK even though neither of the constituents C or K are superconducting by themselves. Furthermore, C_8K exhibits type-I superconductivity when the magnetic field is parallel to the c-axis, and type-II superconductivity when the field is perpendicular to the c-axis. The superconducting transition temperatures, however, tend to be higher for intercalants that are themselves superconducting—KHg and RbHg, for example. One would expect the transition temperature to decrease with increasing stage, consistent with the decrease in the density of electronic states; notable exceptions are the stage-one compounds C_4KHg and C_4RbHg, for which the reported transition temperatures of 0.77 K and 0.99 K, respectively, are lower than the 1.90 K and 1.41 K reported for the corresponding second-stage compounds C_8KHg and C_8RbHg. The critical temperatures are also believed to be sensitive to the in-plane density of the intercalate.

For all superconducting graphite intercalation compounds studied to date, the large anisotropy of the critical magnetic field is well represented by the Ginsburg–Landau theory, a phenomenological theory of superconductivity; the applicability of the Ginsburg–Landau theory is indicative of three-dimensional superconductivity. The large observed anisotropy arises from the fact that the in-plane coherence distance (typically about 2000 Å) is large relative to the c-axis coherence distance (typically about 100 Å). Because the in-plane coherence distance is relatively insensitive to the stage index, while the c-axis coherence distance decreases rapidly with increasing stage, the preparation of higher-stage superconducting graphite intercalation compounds could result in materials that exhibit two-dimensional superconductivity.

I wish to thank Gene Dresselhaus and other current and past members of my research group for many enlightening discussions, and AFOSR for support of my research work through contract number F49620-83-C-0011.

References

1. J. E. Fischer, T. E. Thompson, PHYSICS TODAY, July 1978, page 36.
2. F. R. Gamble, T. H. Geballe, *Treatise on Solid State Chemistry*, N. B. Hannay, ed., Plenum, New York (1976), page 89.
3. *Proceedings of the Conference on Intercalation Compounds of Graphite*, La Napoule, France, 1977, F. L. Vogel, A. Hérold, eds., (Materials Science and Engineering volume 31), Elsevier Sequoia, Lausanne (1977); *Proceedings of the Second Conference on Intercalation Compounds of Graphite*, Provincetown, Mass., 1980, F. L. Vogel, ed., Synthetic Metals **2** (1980); **3** (1981). M. S. Dresselhaus, G. Dresselhaus, Advances in Physics **30**, 139 (1981). *Proceedings of the Yamada Conference IV on the Physics and Chemistry of Layered Materials*, Sendai, Japan, 1980, Y. Nishina, S. Tanuma, H. W. Myron, eds., Physica **105B** (1981). S. A. Solin, Adv. Chem. Phys. **49**, 455 (1982).
4. *Physics of Intercalation Compounds*, L. Pietronero, E. Tosatti, eds., Series in Solid-State Sciences **38**, Springer, Berlin (1981).
5. *Physics and Chemistry of Materials with Layered Structures*, Vol. 6, F. Levy, ed., Reidel, Dordrecht, (1979).
6. A. Hérold in reference 5, page 323.
7. A. Erbil, A. R. Kortan, R. J. Birgeneau, M. S. Dresselhaus, Phys. Rev. B**28**, 6329 (1983).
8. V. L. Pokrovsky, A. L. Talapov, Sov. Phys. JETP **51**, 134 (1980).
9. D. H. McDaniel, P. Boolchand, W. J. Bresser, P. C. Eklund, *Intercalated Graphite*, M. S. Dresselhaus, G. Dresselhaus, J. E. Fischer, M. J. Moran, eds., (Proc. Natl. Materials Res. Soc. Symposia, volume 20), Elsevier-North Holland, New York (1983), page 377.
10. T. Ohno, K. Nakao, H. Kamimura, J. Phys. Soc. Japan. **47**, 1125 (1979).
11. S. Y. Leung, G. Dresselhaus, Phys. Rev. B**24**, 3490 (1981).
12. J. E. Fischer in reference 5, page 481.
13. E. McRae, D. Billaud, J. F. Marêche, A. Hérold, Physica B**99**, 489 (1980).
14. K. Higuchi, H. Suematsu, S. Tanuma, J. Phys. Soc. Japan **48**, 1532 (1980).
15. M. S. Dresselhaus, J.-P. Issi, J. Heremans, Phys. Rev. B**27**, 1333 (1983).
16. F. J. DiSalvo, S. A. Safran, R. C. Haddon, J. V. Waszczak, J. E. Fischer, Phys. Rev. B**20**, 4883 (1979).
17. Yu. S. Karimov, Zh. Eksp. Teor. Fiz. **65**, 261 (1973); M. Suzuki, H. Ikeda, H. Suematsu, Y. Endoh, H. Shiba, M. T. Hutchings, J. Phys. Soc. Japan **49**, 671 (1980).
18. M. Elahy, M. Shayegan, K. Y. Szeto, G. Dresselhaus, Synthetic Metals **8**, 35 (1983).
19. S. Tanuma, Y. Iye, in reference 4, page 298. R. Al-Jishi, Phys. Rev. B**28**, 112 (1983); A. Shimizu, H. Kamimura, Synthetic Metals **5**, 301 (1983). □